Hydrodynamic torque converter operating under dynamic load

P A De La Fuente Bastida[1], H Stoff [2]

Ruhr-University Bochum, Chair of Thermal Turbomachines IC 2-85, 44780 Bochum (Germany)

Abstract— *Unsteady interaction phenomena created by the influence of the blade spacing have been reported in earlier experiments and CFD. However cyclic load changes in start-up and slow-down of the hydrodynamic torque converter operation have been beyond access to the current flow field calculation methods due to the extensive computer run time and memory requirements in the application of time dependent Navier-Stokes solvers to acceleration and deceleration. Therefore computations based on the use of 1D mean-line flow simulation supported by optimised flow correction coefficients tuned in rig-test experiments enable to obtain solutions for engineering-type technical problems.*

Keywords— hydraulic torque converter, automobile.

I. INTRODUCTION

List of symbols	Indices
A cross section of the	P pump
E kinetic energy	S stator
$\vec{C}$ speed of the fluid	T turbine
CFD computational fluid dynamics	1st index number of blade row
J moment of inertia	2nd index inlet or outlet location
$\vec{L}$ swirl, angular momentum	1 inlet of blade row
M torque	2 outlet of blade row
$\vec{R}$ radius vector	
V volume	
d outer diameter	
n revving speed	
t time	
$\eta = \mu\nu = (M_T\, n_T) / (M_P\, n_P)$ = efficiency	
λ conversion number	
μ torque ratio = M_{out} / M_{Pump}	
ν speed ratio n_T / n_P	
ρ density of the fluid	
ω angular velocity	

II. EXPERIENCE FROM THE PAST

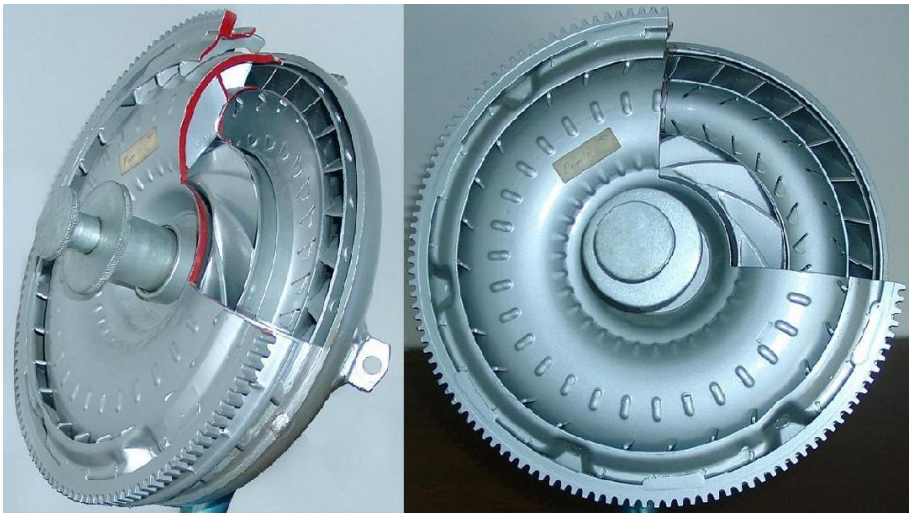

FIGURE 1 VIEW OF THE MODEL W240 AUTOMOTIVE HYDRAULIC TORQUE CONVERTER FABRICATED BY SACHS SHOWING THE EXIT OF THE TURBINE BLADING ON THE OUTER DIAMETER AND THE GUIDE VANE WHEEL DIRECTING THE FLOW FROM TURBINE TO PUMP NEAR THE HUB

The behaviour of hydrodynamic torque converters has been reported by a number of investigators before. R. Herbertz [1] presents a non-linear system of partial differential equations to treat the changing speeds including acceleration and deceleration with the torque converter. E. Rohne [2] compares experiments involving unsteady torque under the presentation of steady-state conditions. He concludes that differences between time-dependent and steady-state results may occur at ratios $\nu = n_T / n_P$ of revving speeds of turbine n_T to pump n_P which can originate from the influence of inertia caused by the rotating mass and an alternating circulation of fluid. In most investigations the moment of inertia of the rotating fluid is neglected because the unsteady phenomena are considered to be quasi-steady. Whenever the changes of the operating speed are slow, the quasi-steady operations fit closely to the description of the mathematically unsteady phenomena. The deceleration can be considered as rapid if 10 m/s^2 is exceeded. Values as high as 120 m/s^2 are attained during the sudden braking to stand-still from a large speed ratio to a small one with the fluid volume being 0.00285m^3.

Steady-state operation of hydraulic torque converters is explained and expressions are defined in VDI 2153 [3]. A set of 4 dimensionless numbers (ν, μ, λ, η) characterises the behaviour of the physical operation from considerations of similarity in incompressible flow. The number μ specifies the torque of the output shaft, driven by the turbine wheel, divided by the torque of the pump attached to the input shaft which drives the operating fluid by centrifugal force through the pump and into the turbine. The coupling of input and output shaft depends on the fluid flow momentum allowing for slip in the transmission. The torque conversion number μ varies over the speed ratio ν which is the ratio of turbine speed over pump speed. The power number λ relates the torque of the pump with the 5th power of the diameter of the turbine rotor wheel the square of the angular speed and the fluid density: $\lambda = (M_{Pump}) / \rho\, \omega^2_{Pump}\, d^5_{Output})$. The efficiency η is the product of the torque conversion number μ and the speed ratio ν representing the power ratio of turbine to pump $\eta = \mu\, \nu = (M_T\, n_T) / (M_P\, n_P)$. The brand name W240 originates from the German word "Wandler" for converter and the outer diameter of the turbine wheel of 240 mm.

Early computer simulations in hydrodynamic torque converters are based on the 1D mean-line flow theory as presented by T. Ishihara [4] and later by R. Leo [5]. The 1D mean-line flow simulation relies on an ensemble of appropriately set coefficients representing total pressure loss and flow angle deviation which did not lead to acceptable results over the entire operating range unless an optimisation algorithm has been used for the data-point-wise adjustment of the ensemble of correction factors setting the difference between the computational result and the test rig result to zero over the entire operating range in repeated sweeps over corrections of deviation angle and total pressure loss. This optimisation is achieved with the algorithm of T. Rechenberg [6] in the computer code by H.P. Prüfer [7].

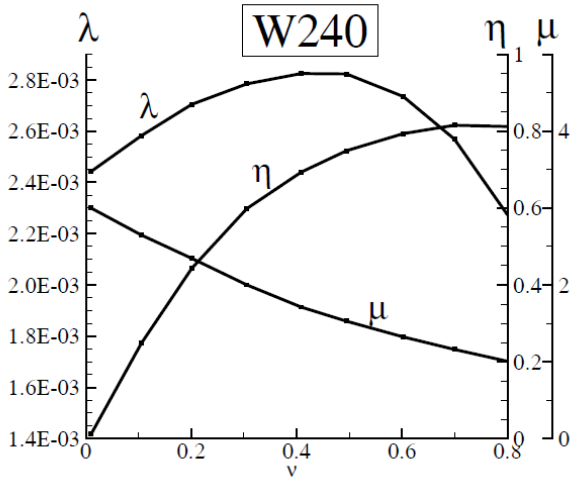

FIGURE 2 FOUR DIMENSIONLESS NUMBERS ARE ν=speed ratio, μ=power number, λ=conversion number and η EFFICIENCY CHARACTERISING THE BEHAVIOUR OF THE PHYSICAL OPERATION FROM CONSIDERATIONS OF SIMILARITY IN INCOMPRESSIBLE FLOW

More refined extensions to unsteady computer formulations are presented by R. Herbertz [1]. Extensive efforts aimed at accessing hydrodynamic torque converter fluid dynamics with Navier Stokes solvers lead originally to the activity in SFB278 [8] dealing with research on hydrodynamic power transmission cumulating finally in the investigation by M.Wollnik et al. [9].

Nevertheless, excessive computer run time requirements in unsteady 3D CFD led the way back to a 1D approach for the problem of unsteady numerical simulation which gives an answer to the original question of SFB278 [8] in which E. Rohne [2] points out a hysteresis effect in the characteristics of the torque converter under steady-state considerations with alternate acceleration and deceleration. He concludes that differences in the characteristics may occur from the influence of inertia of the fluid sloshing about in the blading of the pump and the turbine wheels. Whenever the changes in operating speed are slow the quasi-steady computations fit closely to the description of the experiments in the test rig presented by R. Herbertz [1]. Investigations by P. De La Fuente [10] use the data basis of R. Herbertz [1] for unsteady operation as well as the data of H. J. Förster [11] for steady-state operation in a comparison. R. Herbertz [1] developes the system of equations for the unsteady torque conversion using a mean-line approach involving the rotational speed of the rotor rows and the mass flow balance from an unsteady momentum equation for each of the 3 cascade wheels and the energy conservation equation. In the case under investigation they are rotors of the pump, - of the turbine and of the freewheel, the latter with a speed range restricted to $0.8 < \nu < 1.0$ in which the angle of incidence turns from positive to negative values [12].

Convective angular momentum

$$\frac{d\vec{L}}{dt} = M_i = \frac{d}{dt}\int_{Vi}\left(\vec{R}\times\vec{C}\right)\rho\, dV \tag{1a}$$

$$+ \int_{Ai}\left(\vec{R}\times\vec{C}\right)\rho\vec{C}\, d\vec{A} \tag{1b}$$

momentum in and out of the blade channel

The sum of the angular momentum contributions of pump M_P, turbine M_T and guide vanes M_{Stator} on all bladed wheels must go to zero:

$$M_P + M_T + M_{Stator} = 0 \tag{2}$$

The energy balance requires equilibrium between ingoing power in the pump, outgoing power from the turbine, dissipation by loss as well as the energy variation *dE* with changing speed over the time *dt*:

$$P_{in} + P_{out} + P_{loss} = \frac{dE}{dt} \tag{3}$$

Torque is influenced as well by the mass distribution incorporated in solid parts under rotation at varying speed of constant geometrical shape as by the more complicated case of the changing shape and speed of the volume of the work fluid transmitting the torque. The distribution of the fluid can be lumped into an appropriate shape representing the influence of inertia such as fluid in the shape of a rotating disc, ring or mass concentration positioned on representative radii. The moment of inertia *J* in the volume under rotation can be assumed to be of the shape of a disc with radius r and density ρ:

$$J = \int_{Vi} r^2 \rho \, dV \quad ; \quad M_i = J_i \left(\frac{d\omega_i}{dt} \right) \tag{4}$$

Figures 3 and 7 show the situation with rapid acceleration, 8 and 9 with deceleration as the dimensionless torque rated by the torque M_{P0} and M_{T0} in the instant of the start at the initial moment $t = 0$. In Figures 7 the output shaft is unloaded. In this way the operating point goes from $\nu = 0$ and reaches $\nu = 0.8$ in 2.63 seconds. During the acceleration of ν the motor remains with the pump at constant revving speed (1000 min^{-1}) at $d\omega_P / dt = 0$. In Figure 11 the output shaft undergoes increased loading so that the turbine reaches stand-still in 0.23 seconds. Figures 3 and 11 show torque of the pump and the turbine as well as the speed ratio ν versus time *t*. This allows determining the angular velocities ω_i of pump and turbine by linear interpolation between the data points:

$$\frac{d\omega_i}{dt} \left[\frac{rad}{s^2} \right] = \frac{\left(\omega_{i\,t2} - \omega_{i\,t1} \right) \left[s^{-1} \right]}{\Delta t \, [s]} \tag{5}$$

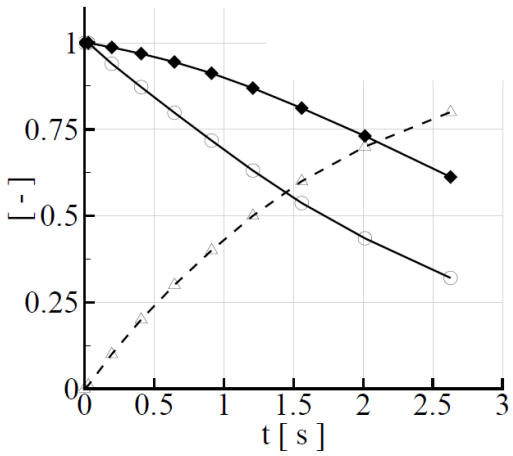

FIGURE 3 Measurement of rated torque M_P/M_{P0} of the pump (-♦-) and of the turbine M_T/M_{T0} (-o-) as well as the speed ratio $\nu = n_T / n_P$ (-Δ-) at unsteady operation measured by R. Herbertz [1] at constant speed of the pump $n_P = 1000\ min^{-1}$ under acceleration of the turbine during t = 2.63 s

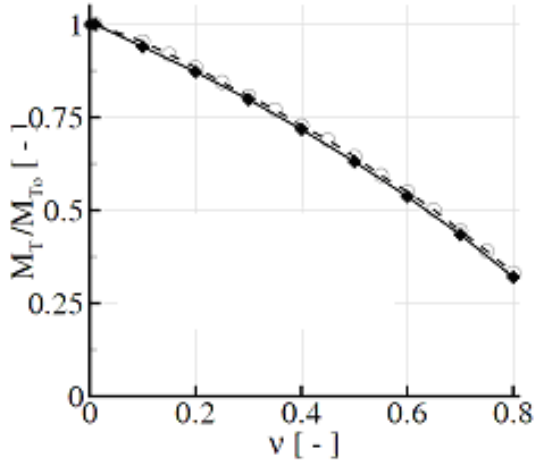

FIGURE 4 Comparison of rated turbine torque M_T/M_{T0} in the unsteady experiment [1] with the steady-state computation. M_{T0} is the initial torque from stand-still to acceleration (measurement -♦- , computation -o-)

The ascend of the velocity ratio ν is assumed to increase linearly between the data points taken during the measurement over time t (Figure 4). In this way it is possible to interpolate the angular speed at each instant between the respective data points. The acceleration changing with time may be described as the instantaneous angular velocity at the time the turbine requires from one data point to the next one.

III. QUASI-UNSTEADY TREATMENT VERSUS TRULY UNSTEADY TREATMENT

In the following the comparison between the characteristics of the reference torque converter W240 with and without the influence of inertia is given as obtained from the transient experiment by R. Herbertz[1] including the moment of inertia as well as excluding it in the tests by H. J. Förster [11] using the steady-state computation.

Figure 4 compares the computed steady-state case with the transient experiment during start-up in 3 seconds. The slower the variations are with time, the better is the agreement [2]. The case of acceleration shows satisfactory agreement between steady as well as unsteady treatment of the turbine. Considerable differences occur between prediction and experiment if the outlet shaft is decelerated to stand-still in *0.23s* from $\nu = 0.8$ to $\nu = 0$. Figures 5a & 5b show a discrepancy between the unsteady experiment (-♦-) and the steady-state computer simulation (-o-) where the latter ignores the moment of inertia of rotating solid parts and fluid matter inside the bladed channel, thus increasing the torque of the turbine (figure 5b) and lowering the torque in the pump (figure 5a) with respect to the 1D computer method for steady-state simulation. An extended theory following interaction of inertia of mass of solid and fluid matter follows the 1D computational aproach with equations by R. Herbertz [1] and is assembled in a MATLAB programme [10].

IV. UNSTEADY COMPUTATION USING THE MEAN-LINE THEORY

The extension of the 1D theory from the steady-state transmission of torque to the unsteady situations of acceleration, deceleration and change of load takes place by the interaction between inertia of rotating mass and fluid as well as the prescribed angular velocities of pump and turbine depending on the time as well as the retarding of pump and turbine wheel under the circumstances of the experimental results of the test rig. Using the optimised loss and deviation corrections with equations (6), (7) and (8) in table 1 below, minor deviations occur in the results of the characteristic curves (figure7).

TABLE 1

MOMENTUM EQUATIONS SOLVED IN THE 1D COMPUTER PROGRAMME FOR PUMP (P), TURBINE (T), STATOR AND FREEWHEEL (S), ANY BLADED WHEEL (I), INERTIA OF SOLID BODY (J) AND FLUID (H)

$r_{11}=r_{32},\ldots r_{21}=r_{12},\ldots r_{31}=r_{22}$

$$M_P = J_P \frac{d\omega_P}{dt} + \rho S_P \frac{dQ}{dt} + \rho Q \left[\left(r^2_{12}\,\omega_P + r_{12}\frac{Q}{A}\cot\beta_{11} \right) - \left(r^2_{11}\omega_P + r_{11}\frac{Q}{A}\cot\beta_{11} \right) \right] \tag{6}$$

$$M_T = J_T \frac{d\omega_T}{dt} + \rho S_T \frac{dQ}{dt} + \rho Q \left[\left(r^2_{22}\,\omega_T + r_{22}\frac{Q}{A}\cot\beta_{22} \right) - \left(r^2_{21}\omega_T + r_{21}\frac{Q}{A}\cot\beta_{21} \right) \right] \tag{7}$$

$$M_S = \rho S_S \frac{dQ}{dt} + \rho Q \left[\left(r_{32}\frac{Q}{A}\cot\beta_{32} \right) - \left(r_{31}\frac{Q}{A}\cot\beta_{31} \right) \right] \tag{8}$$

$$M_i = M_{iJ} + M_{iH} \tag{9}$$

$$M_i = J_i \frac{d\omega_i}{dt} + \rho S_i \frac{dQ}{dt} + \rho Q \left[r_{i_2} \left(r_{i_2}\omega_i + \frac{Q}{A}\cot\beta_{i_2} \right) - r_{i_1} \left(r_{i_1}\omega_i + \frac{Q}{A}\cot\beta_{i_1} \right) \right] \tag{10}$$

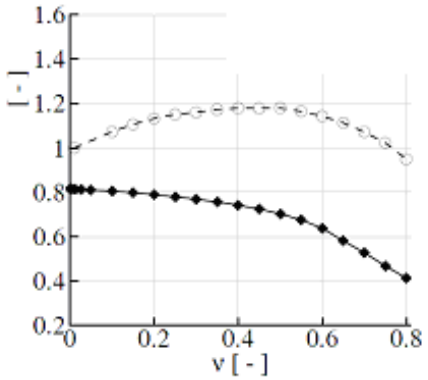

FIGURE 5A

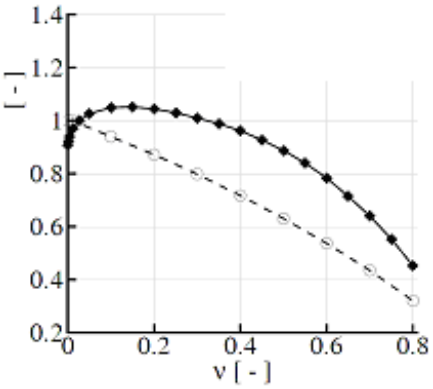

FIGURE 5B

FIGURE 5: Comparison of the rated torques M_P/M_{P0} for the pump (above) and M_T/M_{T0} for the turbine (below) obtained from unsteady measurements (-♦-) and steady-state computation (-o-) with a deceleration of the turbine in 0.23 s from ν=0.8 to ν=0

The hydrodynamic torque is created by the fluid directed in the bladed channel in a way that angular momentum is transmitted. Furthermore the mass of the spinning rotors with the blading and pieces attached to input and output shafts contribute to the amount of torque acting on the shafts as soon as the revving speeds vary. A simple way to take into account the influence of inertia is to add torque from additional rotating angular momentum of solid parts M_{iJ} and rotating fluid matter M_{iH} to consider the dynamic influence.

$$M_i = M_{iJ} + M_{iH} \tag{11}$$

The extension of the 1D theory to allow for unsteady operation including acceleration, deceleration and change of load follows the approach of R. Herbertz [1] and is put down in a MATLAB computer programme solving the equations 6 , 7 and 8 (table 1 below) under the boundary conditions of the time intervals as applied in the experiment making use of the characteristic operating lines of the optimised corrections for loss and deviation fitted to the results of the stationary experiments of the model W240 torque converter in the work by P. De la Fuente [10].

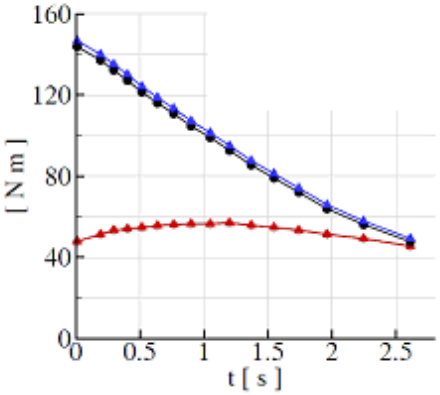

FIGURE 6 A

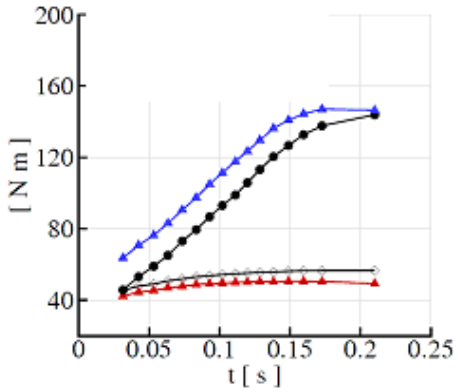

FIGURE 6 B

FIGURE 5: Comparison of 1D-computed torques of the turbine using unsteady (--Δ--) and the steady-state methods (-•-) for the turbine torque M_T under an acceleration of 10 revs/s^2 (above) and of more than 100 revs/s^2 (below) started from time t=0s. The torque of the pump changes less under the unsteady influence (--Δ--, --◊--)

V. SITUATIONS UNDER VARYING LOAD

Under a sudden increase of load on the turbine shaft the motor driving the pump reacts with a modest decrease of angular velocity. The deceleration of the pump remains at a rather constant -30.75m/s^2 (figure 6a). Figure 7 shows a result similar in trend to figure 6a with the torque in the unsteady as well as the steady condition of the accelerating turbine at 10 revs/s^2 but a discrepancy for the deceleration at 100 revs/s^2 starting at t=0 in figure 6b bas well as in figure 9.

The example for the effect of inertia under acceleration shows a fairly similar trend of the rated turbine torque distribution M_T/M_{T0} over the time, no matter how the computational prediction is done by either transient, steady-state, 1D or 3D CFD computation as can be seen in figure 9 and the explanation in figure 14. Contrary to the acceleration in figure 9, the deceleration shows a wide spread in the distribution displayed in figure 10 for the distribution of rated torque over the time t. A rapid slow-down of the output shaft of the turbine causes the disruption of the unidirectional flow as the fluid speed overtakes the turbine wheel speed.

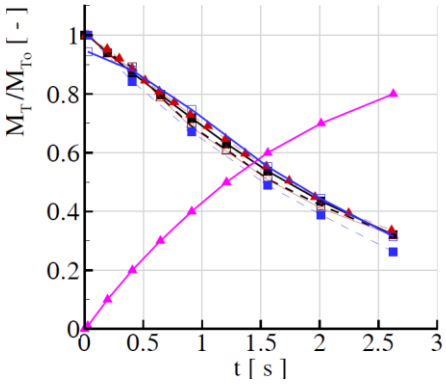

FIGURE 7 Turbine torque M_T/M_{T0} from transient measurements by R. Herbertz [1973] during acceleration from $\nu = 0.01$ to $\nu = 0.8$ in $t = 2.63$ seconds compared with the steady-state measurements by H. J. Förster [11].

- Transient- (—□—) and steady-state measurement (--▲--) .

- 1D transient (--Δ--) and 1D steady-state (—Δ—) computation and

- 3D CFD computation transient (--■--) and steady-state (—□—) by P. De La Fuente [10]

- Ratio of speeds n_T/n_P (—Δ—)

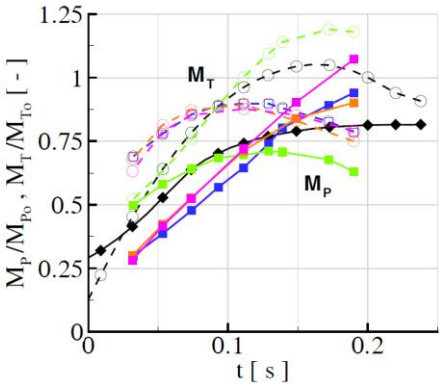

FIGURE 8 Torque of pump (M_P) and turbine (M_T) measured over the time lapse of $t=0.23$ seconds during deceleration from $\nu=0.08$ to $\nu=0.01$ from unsteady measurements by R. Herbertz [1] and steady-state measurement by H. J. Förster [11] in comparison with the 1D- and 3D-computer methods of P. De La Fuente [10] show significant discrepancies in torque M_T/M_{T0} and M_P/M_{P0} during deceleration, in the measurements.

Experiment:

- M_P/M_{P0} transient (—♦—), M_T/M_{T0} transient (--o--) ,

- M_P/M_{P0} steady-state (—□—), M_T/M_{T0} steady-state (--o--) ,

1D computation:

- M_P/M_{P0} steady-state (—■—), M_T/M_{T0} steady-state (--□--)

- M_P/M_{P0} transient (—□—), M_T/M_{T0} transient (--o--) ,

CFD computation:

- M_P/M_{P0} steady-state (—□—), M_T/M_{T0} steady-state (--o--)

- M_P/M_{P0} transient (—□—), M_T/M_{T0} transient (--o--) ,

from P. De La Fuente [10]

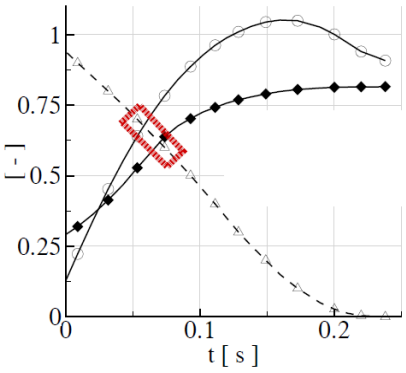

FIGURE 9 Load applied to the output shaft by suddenly retarding the speed ratio from *ν=0.7* down to *ν=0.6* during *0.24* seconds obtained by an unsteady CFD result by P. De La Fuente [10] after a week of central processor time. The rated torque of the pump M_P/M_{P0}(-o-), - of the turbine M_T/M_{T0} (-♦-) and the variation along the speed ratio ν(-Δ-) are shown over the time t

VI. CONCLUSION

In the steady-state CFD analysis by M.Wollnik et al. [9] performance in computational effort required 1.4 Million elements. in the unsteady case. In the present 3D CFD simulation only 676 711 elements had been used for the simulation of a single blade channel in figure 8 and 9. Computer time of the order of one week central processor time had been required for the run indicated in figure 9 from *ν=7* down to *ν=6* during *0.24* seconds. Once the optimisation procedure has set the calibration coefficients correcting flow angle and pressure loss of the 1D method in the curve fit to preceding rig tests, the 1D performance prediction is applicable to the prediction of any torque converter of identical blade shapes and fluid mass at moderate computing times with better accuracy for the situation of acceleration than of deceleration (figures 7 and 8).

At present the truely unsteady analysis on the basis of 3D Navier-Stokes solvers for the torque converter case does not seem economically justified for engineering applications because of excessive computer time requirement.

ACKNOWLEDGEMENTS

The authors gratefully acknowledge the support by Professor R.Mönig in co-chairing the work of the first author and Professor R.Mailach in enabling the administrative conditions to bring this task to success. Doctors M.Wollnik, W.Volgmann and H.P.Prüfer attributed components of the software. The exchange students A. Sánchez-Arjona Rengel as well as J.J.Sánchez-Migallón López contributed to the programming of the MATLAB code. The authors acknowledge the contribution of a fellowship by DAAD (German organisation for the international exchange of students) providing funding for the first author.

REFERENCES

[1] Herbertz R., Untersuchung des dynamischen Verhaltens von Föttinger-Getrieben, Dissertation Universität Hannover 1973

[2] Rohne E., Verhalten von Föttinger-Wandlern bei Laständerungen und Schwingungsvorgängen, Antriebstechnik 22, Nr 12: S. 37-41, 1983

[3] VDI 2153, "Hydrodynamische Leistungsübertragung - Begriffe, Bauformen, Wirkungsweise", Düsseldorf: Beuth Verlag GmbH [1994]. Verein Deutscher Ingenieure - Handbuch Getriebetechnik II Richtlinie 2153

[4] Ishihara T., A Study of Hydraulic Torque Converters. Technical report, Report University of Tokyo, 1955.

[5] Leo R., Eindimensionale Kennlinienberechnung hydrodynamischer Wandler, Ruhr-Universität Bochum, Lehrstuhl für Fluidenergiemaschinen, Diplomarbeit 1990 (unpublished)

[6] Rechenberg I., Evolutionsstrategie, Optimierung technischer Systeme nach Prinzipien der biologischen Evolution, Friedrich Frommann Verlag, Stuttgart,1973

[7] Prüfer, H.P., Parameteroptimierung, ein Werkzeug des rechnergestützten Konstruierens, Ruhr-Universität Bochum, Fakultät für Maschinenbau, Konstruktionstechnik 1988

[8] SFB278, Sonderforschungsbereich 278 "Hydrodynamische Leistungsübertragung", Abschlußbericht, Ruhr-Universität Bochum, Fakultät für Maschinenbau, Berichtszeitraum 1990-1995

[9] Wollnik, M.; Volgmann, W.; Stoff, H.Importance of the Navier-Stokes Forces on the Flow in a Hydrodynamic Torque Converter. Paper No.538-175 Proceedings of the 4th WSEAS International Conference on Fluid Mechanics and Aerodynamics, Elounda, Greece, August 21-23, 2006; Ed.'s: Catrakis, H.J.; Sohrab, S.H.; Necasova, S.; pages 168-173, ISSN 1790-5095; ISBN 960-8457-52-1

[10] De la Fuente Bastida, P. A., Die CharakteristikeneinesTrilok-Drehmomentwandlers unter stetiger und dynamischer Last, Dissertation Ruhr-Universität Bochum, Lehrstuhl für Thermische Turbomaschinen 2012

[11] Förster H. J., Automatische Fahrzeuggetriebe: Grundlagen, Bauformen, Eigenschaften, Besonderheiten, Springer Verlag Berlin, November 1990

[12] Ackermann, J.F., Experimentelle und numerische Strömungsuntersuchung eines Trilok-Drehmomentwandlers mit schmaler Kreislaufform, Dissertation Ruhr-Univ.Bochum 2001, Fluidenergiemaschinen, Fortschr.-Ber. VDI,Reihe 7, Nr.421, Düsseldorf: VDI-Verlag 2001